A study on the sensitivity of the K-EUSO and the Mini-EUSO missions to the detection of EECRs

Marta Bianciotto

Università degli Studi di Torino

IMPRS Recruitment Workshop
July 18th, 2022

UNIVERSITÀ DEGLI STUDI DI TORINO

INFN

The JEM-EUSO program to study EECRs

JEM-EUSO: Joint Experiment Missions for Extreme Universe Space Observatory

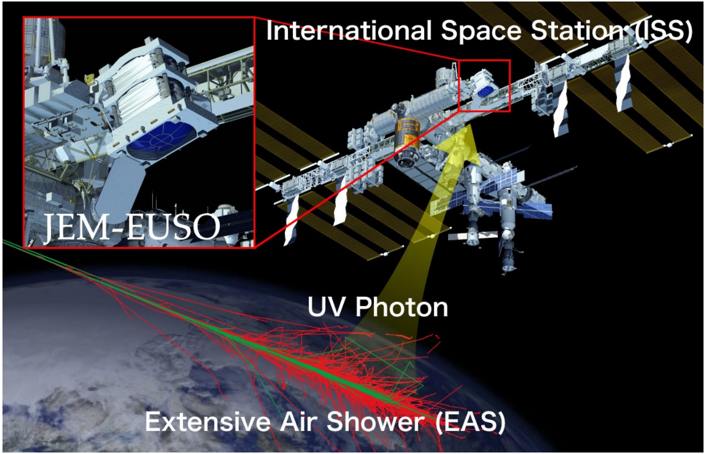

⟶ Focus on Mini-EUSO & K-EUSO

The Mini-EUSO mission

Mini-EUSO is installed on the UV-transparent window in the Zvezda module of the ISS ($37 \times 37 \times 62\,\mathrm{cm}^3$ dimension constraints) $\rightarrow$ CRs detection not possible

Mini-EUSO telescope:

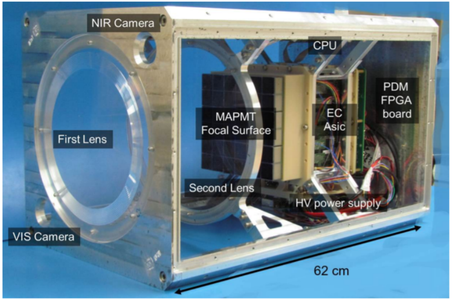

But Mini-EUSO is able to address different phenomena:

- Emulated CRs (1 GTU $= 2.5\,\mu\mathrm{s}$, trigger L1)
- Atmospheric phenomena
- Nocturnal UV emissions/background

$\longrightarrow$ First dynamic map of nocturnal UV emissions in Earth's atmosphere

The K-EUSO mission

- Intermediate step between Mini-EUSO and POEMMA
- First mission of EUSO family capable of EECRs detection from space
- Planned to fly in 2025+ (Russian segment of the ISS)

K-EUSO telescope and focal surface:

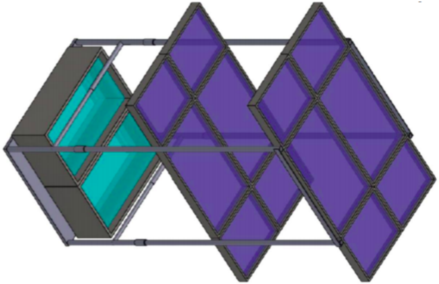

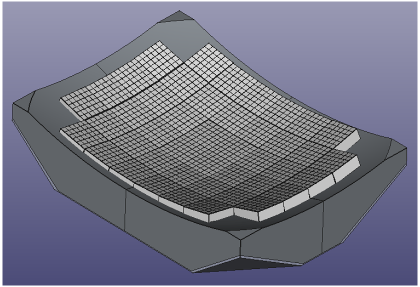

ESAF

- ESAF is the EUSO Simulation and Analysis Framework
- Based on C++ object oriented and ROOT (CERN)
- Produces 2 executable: Simu and Reco

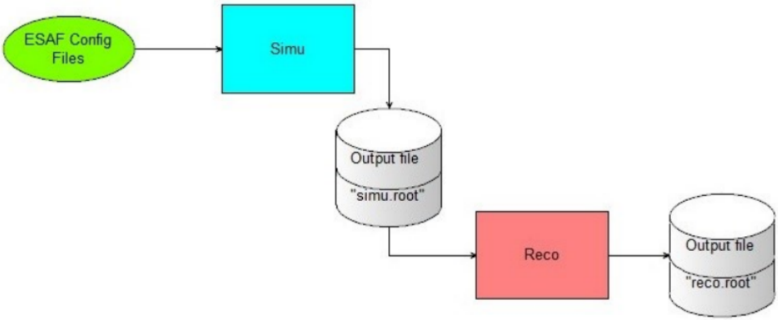

⟶ Simu simulates the events and the detector response. Reco analyses the output of the simulation and reconstructs the events. The two programs are independent.

K-EUSO trigger efficiency

- $N = 4500$ showers, $E = 10^{19} - 10^{20.5}$eV, $\theta = 0^\circ - 90^\circ$
- $\epsilon(E) = \frac{N_{trigg}}{N_{simu}}(E)\frac{A_{simu}}{A_{fov}}$

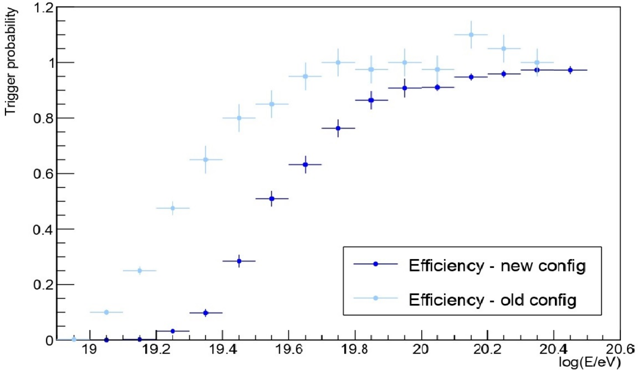

$\longrightarrow$ Energy threshold $\sim 3 \times 10^{19}\,\mathrm{eV}$

$\longrightarrow$ Full $\epsilon \sim 1 \times 10^{20}\,\mathrm{eV}$

K-EUSO annual exposure

- $N = 4500$ showers, $E = 10^{19} - 10^{20.5}$eV, $\theta = 0^\circ - 90^\circ$
- $\mathcal{E}(E) = \frac{N_{trigg}}{N_{simu}}(E) \times A_{simu} \times \Omega \times \eta \times \eta_{clouds} \times \eta_{city} \times t$

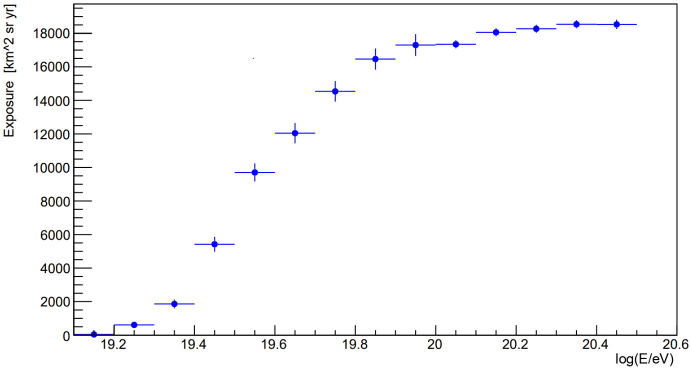

$\longrightarrow$ Exposure $\sim 18\,000\,\mathrm{km}^2$ sr year at the plateau

K-EUSO expected rate of triggered events

Assuming Auger spectrum and K-EUSO trigger efficiency, the expected rate of triggered events:

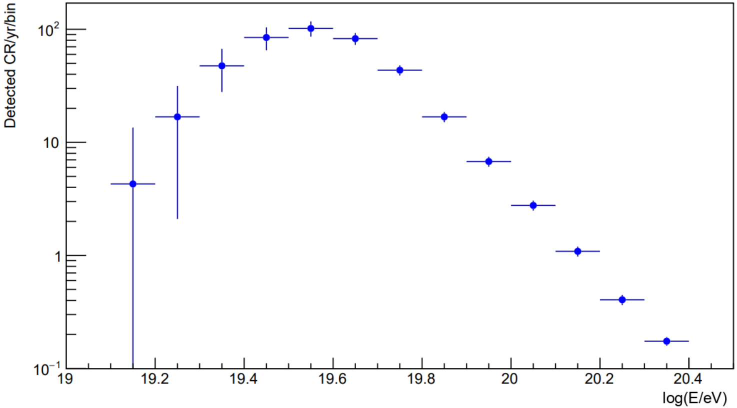

- 4 events/year above 1×10^{20} eV $\longrightarrow$ 4 times Auger
- 65 events/year above 5×10^{19} eV $\longrightarrow$ 2 times Auger

K-EUSO angular reconstruction performance

- 500 showers simulated in the center of the detector
- Fixed conditions: $E = 1 \times 10^{20}\,\mathrm{eV}$, $\theta = 45° - 60°$

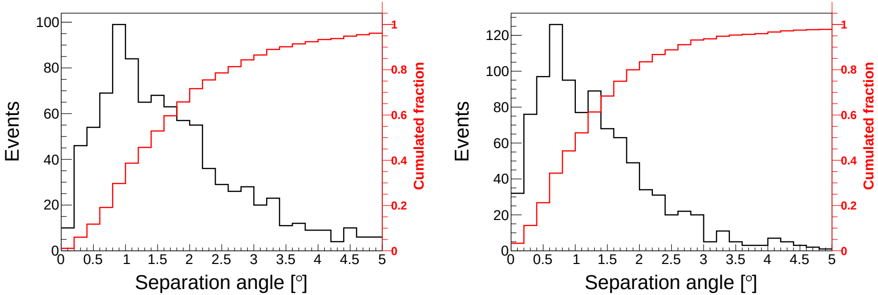

1. Black curve: histogram of the separation angle between the real direction and the reconstructed direction
2. Red curve: integral of the events distribution from 0 to $\infty \longrightarrow$ the angular resolution is calculated as the angle within which 68% of the events fall (γ_{68})

K-EUSO angular reconstruction performance

- 500 showers simulated in 16 combinations of energy and zenith angle both for the center and the field of view
- The angle within which 68% of the events fall (γ_{68}) is plotted as resolution

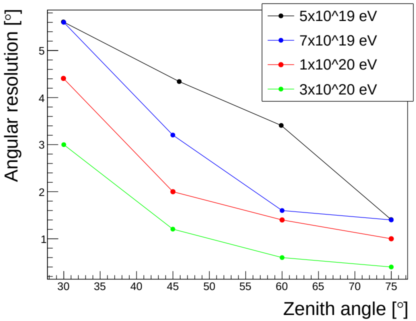

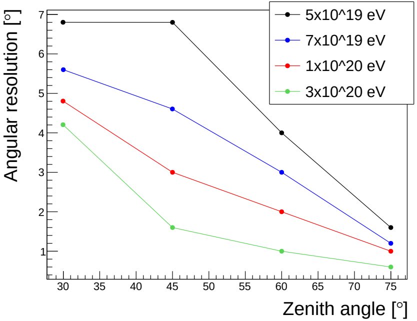

1. Left: center of the field of view $\longrightarrow 3^\circ - 7^\circ$ for low zenith angles up to $1^\circ - 2^\circ$ for high zenith angles, better performance as the energy increases
2. Right: full field of view

K-EUSO energy reconstruction performance

- 2500 showers simulated in the center of the detector
- Fixed conditions: $E = 1 \times 10^{20}\,\mathrm{eV}$, $\theta = 60°$

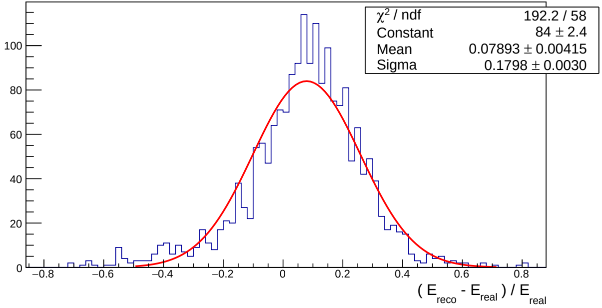

1. $(E_{\mathrm{reco}} - E_{\mathrm{real}})/E_{\mathrm{real}}$ distribution
2. Energy resolution evaluated as the standard deviation of the distribution (gaussian fit in $\pm 3\sigma$ range)
3. Biases in energy reconstruction: automatic fit, gaps, geometry

K-EUSO energy reconstruction performance

- 2500 showers simulated at fixed energies and zenith angles both for the center and the field of view

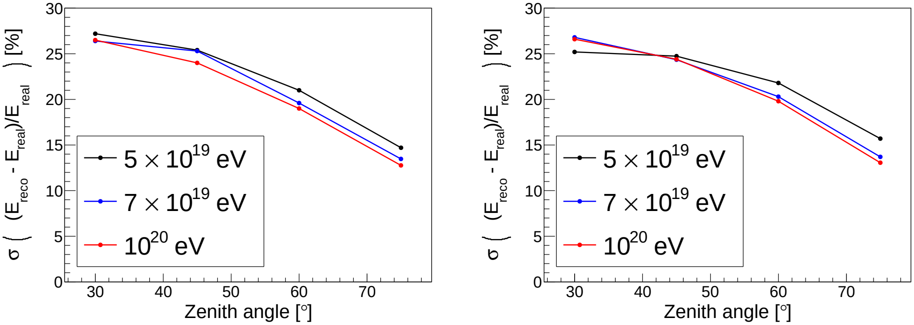

1. Left: center of the field of view $\longrightarrow$ 25% for low zenith angles up to 15% for high zenith angles, better performance as the energy increases
2. Right: full field of view

K-EUSO X_{max} reconstruction performance

- X_{max} = depth of maximum development of the shower, important for cosmic rays composition
- 4500 showers simulated in the center of the detector
- Fixed conditions: $E = 2 \times 10^{20}\,\mathrm{eV}$, $\theta = 30°$

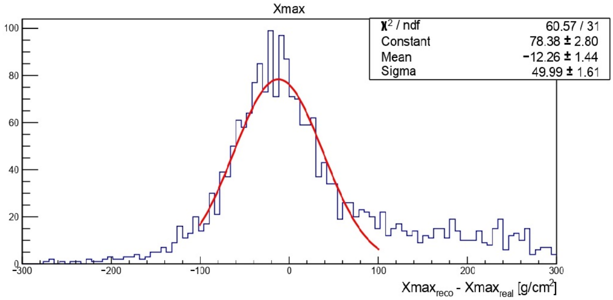

1. $(X_{max,reco} - X_{max,real})$ distribution
2. X_{max} resolution evaluated as the standard deviation of the distribution (gaussian fit of the central peak) $\rightarrow$ exclusion of the tails

K-EUSO X_{max} reconstruction performance

Center of the detector

Energy [eV]	Zenith angle [°]	Xmax resolution $[g/cm^2]$
7×10^{19}	30	81
7×10^{19}	45	92
1×10^{20}	30	63
1×10^{20}	45	71
2×10^{20}	30	50
2×10^{20}	45	60

Full field of view

Energy [eV]	Zenith angle [°]	Xmax resolution $[g/cm^2]$
2×10^{20}	45	60

Mini-EUSO trigger efficiency in uniform/disuniform bg

- Study of Mini-EUSO L1 trigger efficiency in uniform/disuniform background $\rightarrow$ relevant for future space-based experiments like K-EUSO
- 1 count/pixel/GTU, $\sim$ 500 photons per m^2srns (average)
- $\eta_Q = 0.27$ (average)

Disuniform background

- Obtained in ESAF by simply re-scaling the η_Q of each pixel
- But disuniformity may be due to clouds/different geographical conditions

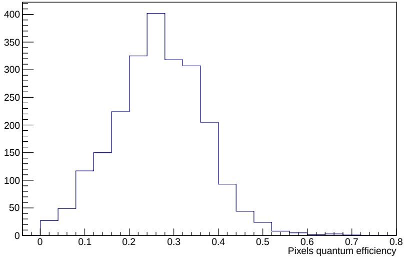

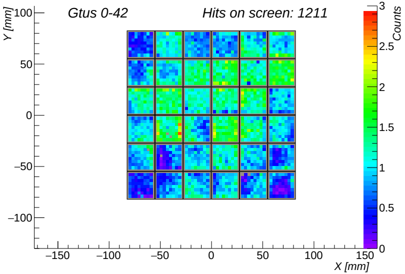

Mini-EUSO trigger efficiency in uniform/disuniform bg

- $N = 10^4$ showers, $E = 10^{21} - 10^{22}$eV, $\theta = 0° - 90°$
- $\epsilon(E) = \frac{N_{trigg}}{N_{simu}}(E)\frac{A_{simu}}{A_{fov}}$
- Fit with error function: $\epsilon(E) \sim \frac{1}{2}[1 + erf(\frac{log_{10}(E/eV) - p_0}{p_1})]$

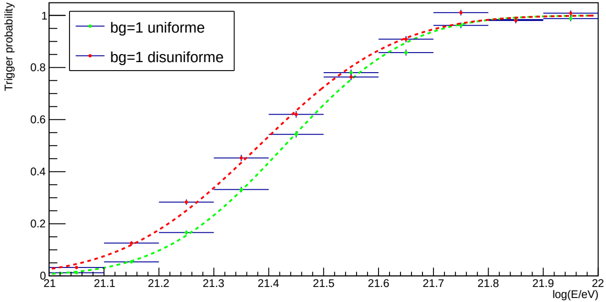

- Threshold: $E_{th} \sim 2.5 \times 10^{21}\,\mathrm{eV}$ (uniform) vs $E_{th} \sim 2 \times 10^{21}\,\mathrm{eV}$ (disuniform)
- Plateau: $E_{Full} \sim 6 \times 10^{21}\,\mathrm{eV}$

Mini-EUSO trigger efficiency vs bg counts

Uniform background, increased counts/pixel/GTU:

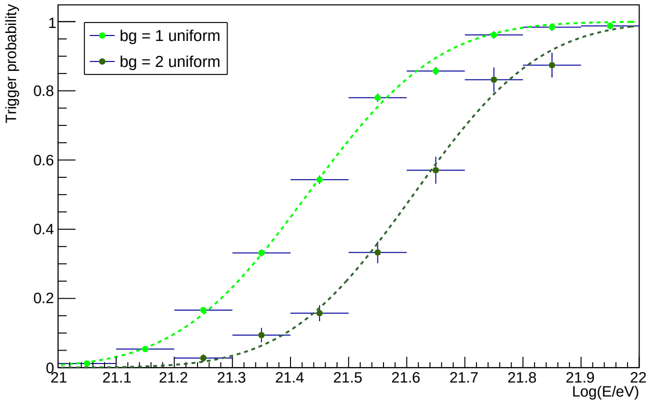

$\longrightarrow$ The energy threshold scales as $\sqrt{2}$

Mini-EUSO trigger efficiency vs bg counts

Disuniform background, increased counts/pixel/GTU:

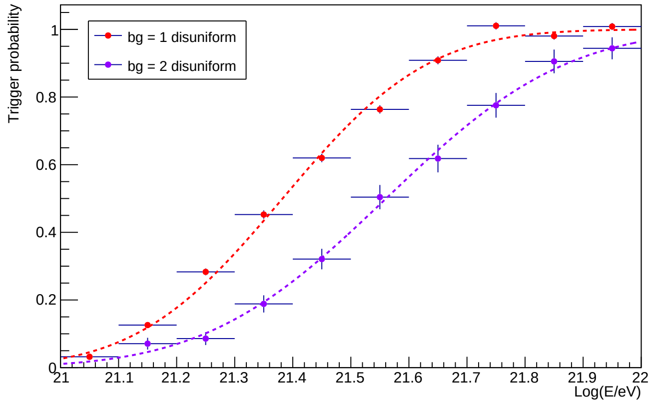

$\longrightarrow$ The energy threshold scales as $\sqrt{2}$

Conclusions

- **K-EUSO expected performance**
  - Expected rate of triggered events $\longrightarrow$ $2\times$ Auger ($E > 5 \times 10^{19}$ eV)
  - Angular resolution $\longrightarrow 1^\circ - 7^\circ$
  - Energy resolution $\longrightarrow$ 15% - 25%
  - X_{max} resolution $\longrightarrow 50\,\mathrm{g/cm^2} - 90\,\mathrm{g/cm^2}$
- **Mini-EUSO expected performance**
  - No drop in trigger performance if the background is disuniform $\longrightarrow$ positive result in view of future space-based missions like K-EUSO
  - The energy threshold scales as the $\sqrt{}$ of bg counts

Thanks for your attention!

BACKUP SLIDES

INTRODUCTION

JEM-EUSO to study EECRs

EECRs: $E > 5 \times 10^{19}\,\mathrm{eV}$, $\phi \sim 1\,\mathrm{particle/km^2/century} \longrightarrow$ only few events per year with ground experiments.

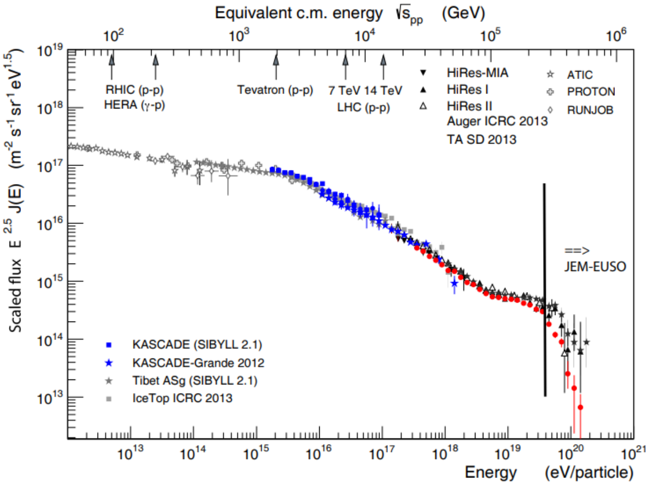

JEM-EUSO to study EECRs

Open problems:

- Origin of EECRs
- Discrepancies of data from the two hemispheres at the end of the spectrum

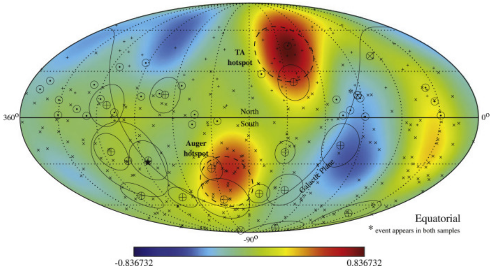

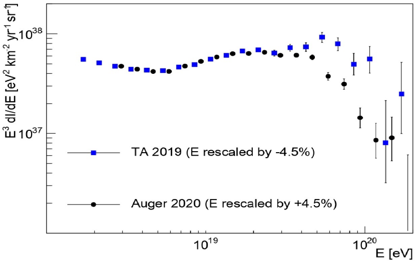

Space mission (JEM-EUSO):

- More statistics
- Flat exposure over full sky

Cosmic Ray interaction in atmosphere

The primary interacts with the atmosphere and produces secondary particles (EAS, Extensive Air Showers).

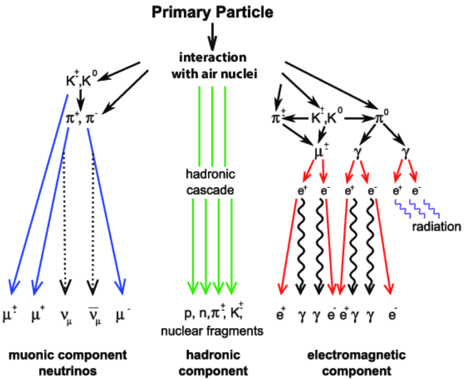

Figure: Interaction of the primary in atmosphere.

Three components:

- Muonic
- Hadronic
- Electromagnetic

Hadronic and electromagnetic components closer to the core.

JEM-EUSO telescope

- Fast, high-pixelized, large aperture and large field of view digital camera
- Near-UV wavelength range (300-400 nm)
- Time resolution 2.5 μs
- Spatial resolution 0.75 km
- Determination of energy and direction of the primary particles

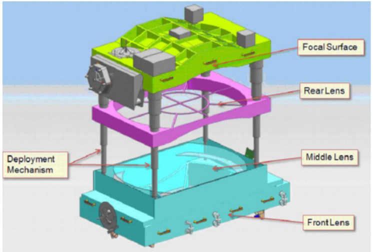

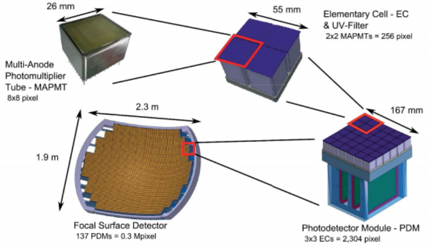

Figure: Left: Conceptual view of the JEM-EUSO telescope. Right: Schematic view of the focal surface and it's components.

JEM-EUSO instrument parameters

Instrument parameters

Field of view	$\pm 30^\circ$
Aperture diameter	$2.5\,\mathrm{m}$
Optical bandwidth	$30 - 400\,\mathrm{nm}$
Angular resolution	0.1°
Pixel size	$4.5\,\mathrm{mm}$
Number of pixels	$\sim 2 \times 10^5$
Pixel size at the ground	$550\,\mathrm{m}$
Duty cycle	$20 - 25\%$
Observational area	$2 \times 10^5\,\mathrm{km}^2$

JEM-EUSO mission parameters

Mission parameters

Mass	$1896\,\mathrm{kg}$
Power	$998\,\mathrm{W}$
Data transfer	$297\,\mathrm{bps}$
Height of the orbit	$\sim 430\,\mathrm{km}$
Inclination of the orbit	51.6°

K-EUSO instrument and mission parameters

Instrument parameters

Field of view	$\pm 20^\circ$
Observational area	$180 \times 260\,\mathrm{km}^2$
Optical bandwidth	$300 - 400\,\mathrm{nm}$
Focal surface area	$1.3\,\mathrm{m}^2$
Number of pixels	101,376
Pixel size	$3 \times 3\,\mathrm{mm}$
Pixel field of view	0.1°
Event time sampling	$1 - 2.5\,\mu\mathrm{s}$
Duty cycle	$\sim 20\%$

Mission parameters

Operation period	6 years
Launching rocket	Soyuz
Module	MRM-1
Mass	$500\,\mathrm{kg}$
Power (operative)	$300\,\mathrm{W}$
Power (non-operative)	$100\,\mathrm{W}$
Data transfer rate	$100\,\mathrm{kbps}$
Altitude	$\sim 400\,\mathrm{km}$
Orbital inclination	51.46°

Mini-EUSO instrument and mission parameters

Instrument and mission parameters

Mass	30 kg
Size	35 cm × 35 cm×60 cm
Power	30 W
Voltage	28 V
Temporal resolution	2.5 μs
Spatial resolution	$\sim$ 6 km
Field of view	±19°
Lenses diameter	25 cm
Lenses thickness	8 mm

Mini-EUSO & K-EUSO

Mini-EUSO mission

Mini-EUSO is installed on the UV-transparent window in Zvezda module of the ISS $\longrightarrow$ $37 \times 37 \times 62\,\mathrm{cm}^3$ dimension constraints $\longrightarrow$ **NO CRs DETECTION!**

But Mini-EUSO is able to address different phenomena:

- D1 timescale ($= 2.5\,\mu\mathrm{s} = 1$ GTU) dedicated to emulated cosmic rays signals (L1 trigger)
- D2 timescale ($= 320\,\mu\mathrm{s}$) dedicated to various atmospheric phenomena such as TLEs, ELVES and meteors (L2 trigger)
- D3 timescale ($= 40.96\,\mathrm{ms}$) dedicated to nocturnal UV emissions in Earth's atmosphere (no trigger)

$\rightarrow$ **First dynamic map of nocturnal UV emissions in Earth's atmosphere**

Mini-EUSO telescope

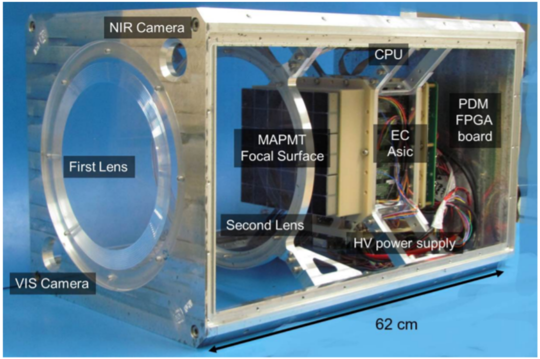

- Optics: 2 Fresnel lenses (25 cm diameter) with wide field of view
- FS: matrix of 36 Multi-Anode Photomultiplier Tubes (MAPMTs) arranged in an array of 6×6 elements $\longrightarrow$ one PDM

K-EUSO telescope

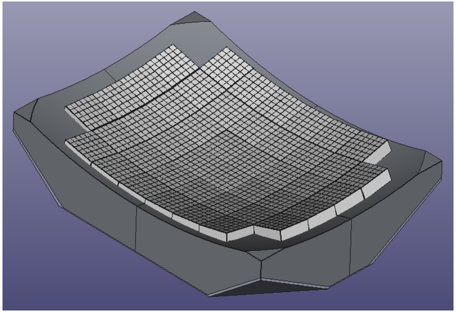

- Optics: 2 Fresnel lenses that focus the light onto a FS $1300 \times 1000\,\mathrm{mm}^2$
- FS: 44 PDMs (vs 52 PDMs in old configuration) of 36 MAPMTs each
- MAPMT: 64 independent channels/pixels $3\,\mathrm{mm}$ size
- Each channel has $0.1°$ FoV $\sim 700\,\mathrm{m}$ on the ground
- Time resolution from $1\,\mathrm{\mu s}$ to $2.5\,\mathrm{\mu s}$ ($2.5\,\mathrm{\mu s} = 1 GTU$ considered in my analysis)

ESAF

Simulation

- Simulation of the entire physical process from shower to telemetry
- Possibility to add background
- Trigger and several algorithms for each detector

Example of a 10^{20} eV, 60° event simulated by ESAF:

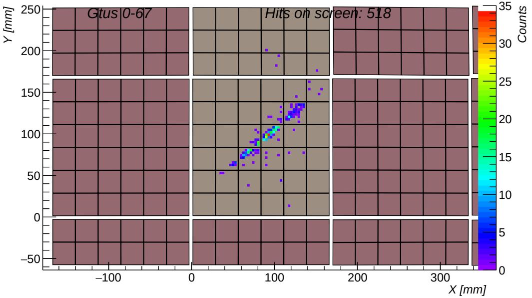

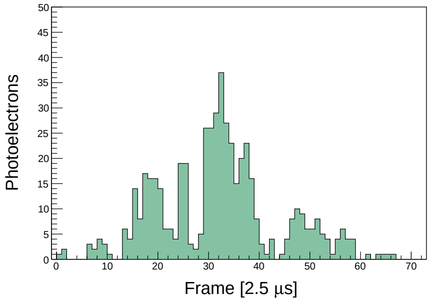

Reconstruction

- Recognize the signal of the shower
- Pattern recognition: PWISE/LTT $\longrightarrow$ both algorithms looking for signal excesses concentrated in space and moving in a coherent way
- Direction reconstruction (θ, ϕ)
- Profile reconstruction (E, X_{max})

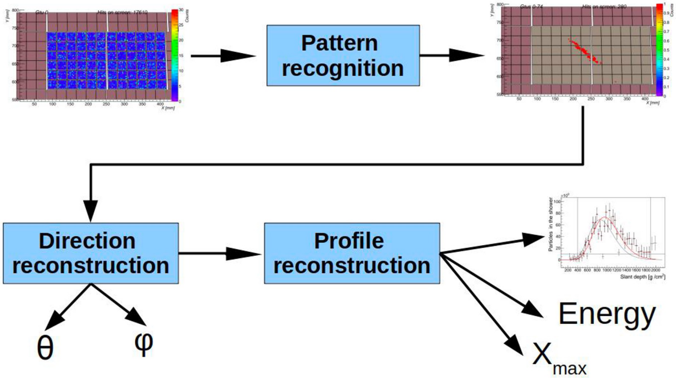

ESAF - Reconstruction scheme

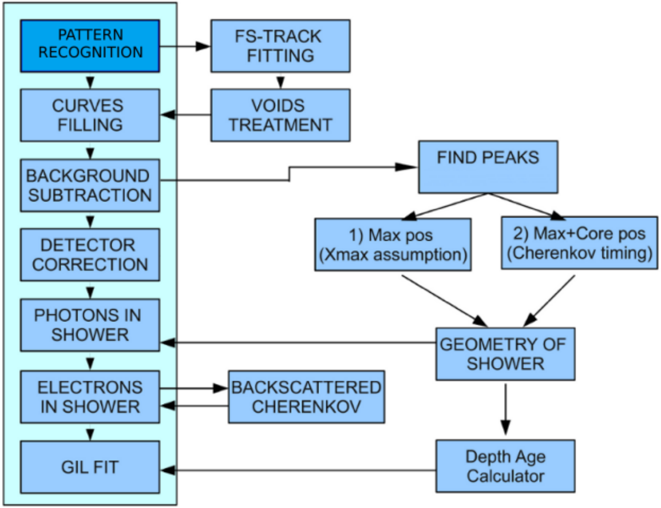

ESAF - X_{max} reconstruction

- X_{max} = depth of maximum development of the shower, important for cosmic rays composition

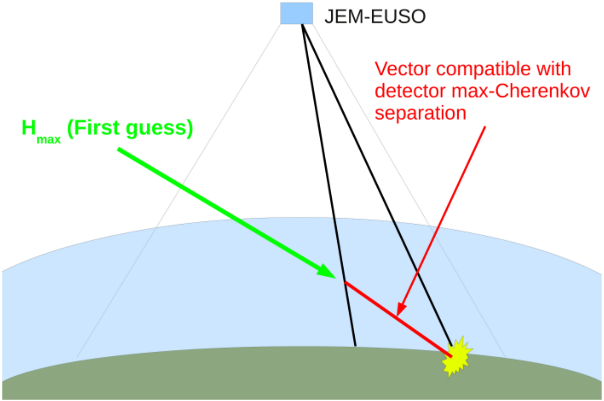

→ Identification of Cherenkov mark makes possible to calculate the altitude of the maximum

LTT technique for E reconstruction

- Linear Tracking Trigger (LTT)
- Selects pixels on focal surface containing the highest number of counts, then searches for the track that maximizes counts by moving an integration box along a predefined set of directions intersecting this point

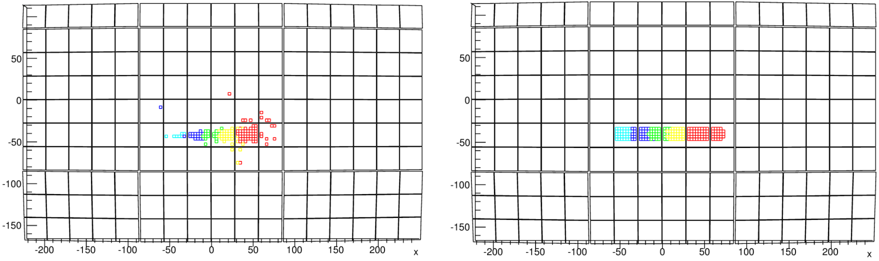

Figure: Left: The evolution in time of the shower simulated track. The color scale represents 5 different time windows in which simulated photons reach the detector. Right: The signal selection according to the *LTTPatternRecognition* algorithm. In color scale, 5 time windows each of 10 GTUs can be seen.

PWISE technique for direction reconstruction

- Peak and Window Searching (PWISE)
- Only considers pixels whose peak is above threshold, then searches for time window with the highest SNR and if the SNR is above threshold photon-counts within time window that maximizes SNR are selected

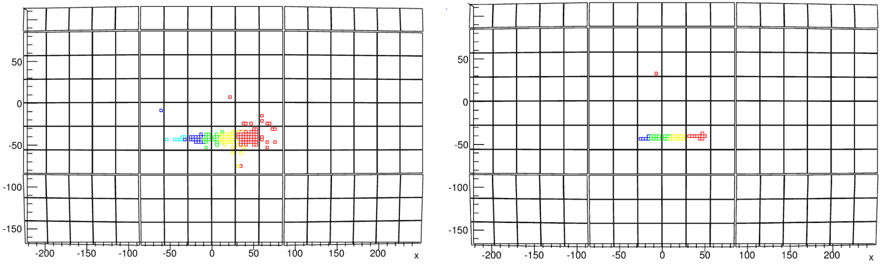

Figure: Left: The evolution in time of the shower simulated track. The color scale represents 5 different time windows in which simulated photons reach the detector. Right: The signal selection according to the PWISE algorithm. In color scale, 5 time windows each of 10 GTUs can be seen.

ANGULAR RECO

K-EUSO angular resolution (center)

Center of the field of view

Energy [eV]	Zenith angle [°]	γ_{68} [°]
5×10^{19}	30	5.6
5×10^{19}	45	4.4
5×10^{19}	60	3.4
5×10^{19}	75	1.4
7×10^{19}	30	5.6
7×10^{19}	45	3.2
7×10^{19}	60	1.6
7×10^{19}	75	1.4
1×10^{20}	30	4.4
1×10^{20}	45	2.0
1×10^{20}	60	1.4
1×10^{20}	75	1.0
3×10^{20}	30	3.0
3×10^{20}	45	1.2
3×10^{20}	60	0.6
3×10^{20}	75	0.4

K-EUSO angular resolution (full field of view)

Full field of view

Energy [eV]	Zenith angle [°]	γ_{68} [°]
5×10^{19}	30	6.8
5×10^{19}	45	6.8
5×10^{19}	60	4
5×10^{19}	75	1.6
7×10^{19}	30	5.6
7×10^{19}	45	4.6
7×10^{19}	60	3
7×10^{19}	75	1.2
1×10^{20}	30	4.8
1×10^{20}	45	3
1×10^{20}	60	2
1×10^{20}	75	1
3×10^{20}	30	4.2
3×10^{20}	45	1.6
3×10^{20}	60	1
3×10^{20}	75	0.6

BIASES IN E_{RECO}

Biases in E_{reco} - $1 \times 10^{20}\,\mathrm{eV}$, 60°

- $N = 100$ showers
- $E = 1 \times 10^{20}\,\mathrm{eV}$
- $\theta = 60$ degrees
- Center of the FOV

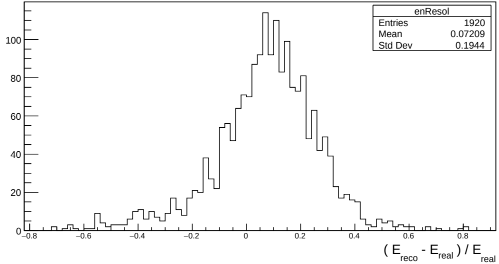

$\longrightarrow \sim +7\%$ bias.

Figure: $(E_{\mathrm{reco}} - E_{\mathrm{real}})/E_{\mathrm{real}}$ distribution of 2000 $1 \times 10^{20}\,\mathrm{eV}$, 60 degrees events simulated in the center (for this analysis we only consider 100).

Biases in energy reconstruction

Bias in E_{reco}: (1) Automatic fitting procedure

→ Event per event study

→ $N = 100,\ E = 1 \times 10^{20}\,\mathrm{eV},\ \theta = 60^\circ$

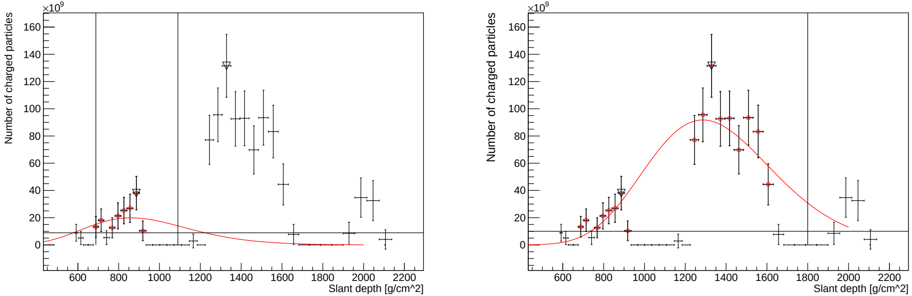

→ Possible optimization event per event for better performance

→ 20% of fits corrected

Biases in energy reconstruction

Bias in E_{reco}: (2) Geometry reconstruction

→ Test with fixed geometry

→ $N = 100$, $E = 1 \times 10^{20}\,\mathrm{eV}$, $\theta = 60^\circ$

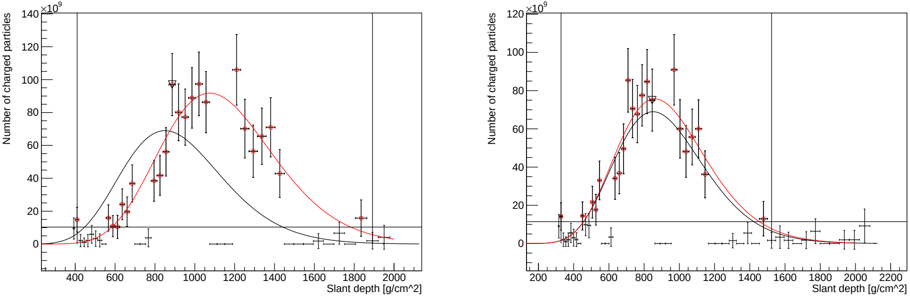

→ Geometry reconstruction can be optimized

→ Not resolutive in all cases

Biases in energy reconstruction

Bias in E_{reco}: (3) PMTs/PDMs gaps

→ Event per event study

→ $N = 100,\ E = 1 \times 10^{20}\,\mathrm{eV},\ \theta = 60°$

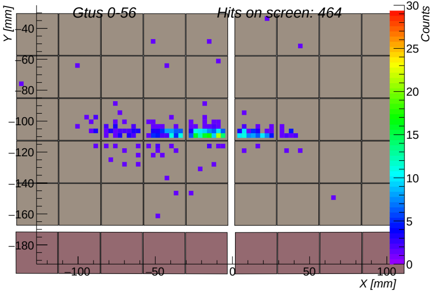

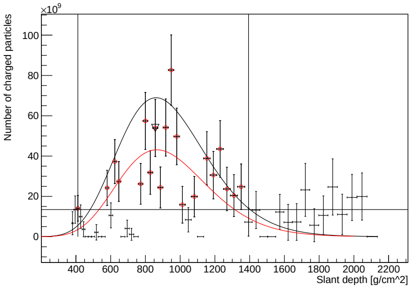

→ Still causes underestimation/overestimation of E_{reco} in 10% of optimized events (ideal geometry reconstruction + fits correction)

→ Unfortunately not fixable

BIASES IN E_{RECO} -EVENTS CLASSIFICATION

Biases in E_{reco} - 1×10^{20} eV, 60°

- $N = 100$ showers
- $E = 1 \times 10^{20}$ eV
- $\theta = 60$ degrees
- Center of the FOV

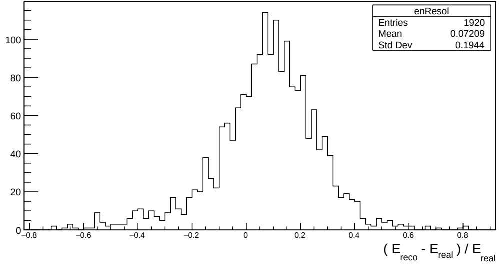

Figure: $(E_{\rm reco} - E_{\rm real})/E_{\rm real}$ distribution of 2000 1×10^{20} eV, 60 degrees events simulated in the center (for this analysis we only consider 100).

$\longrightarrow \sim +7\%$ bias.

Events classification

Different biases in reconstruction for different types of shower?

1. Classification of events from shower profiles in 4 categories
   $\rightarrow$ A, B, C, D = good, half-good, half-bad, bad
2. Calculate $(E_{\mathrm{reco}} - E_{\mathrm{real}})/E_{\mathrm{real}}$ for each event
3. Calculate the average bias and uncertainty for each category

Biases in E_{reco} - $1 \times 10^{20}\,\mathrm{eV}$, 60° example

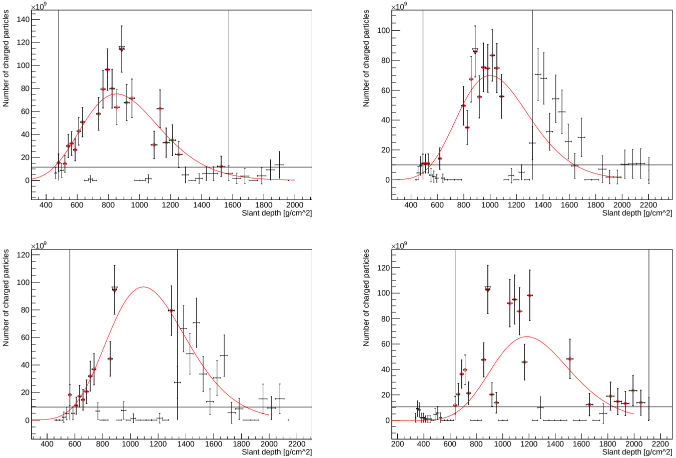

Figure: Examples of shower profiles belonging to different categories. Top left: A ($\delta E = 0.09$). Top right: B ($\delta E = 0.1$). Bottom left: C ($\delta E = 0.4$). Bottom right: D ($\delta E = -0.05$).

Biases in E_{reco} - $1 \times 10^{20}\,\mathrm{eV}$, 60° example

Type A events		Type B events	
Number of events	24	Number of events	38
Overstimated E_{reco}	20	Overstimated E_{reco}	25
Underestimated E_{reco}	4	Underestimated E_{reco}	13
Average δE	14.8 %	Average δE	7.1 %
Type C events		**Type D events**	
Number of events	19	Number of events	16
Overstimated E_{reco}	15	Overstimated E_{reco}	5
Underestimated E_{reco}	4	Underestimated E_{reco}	11
Average δE	14.5 %	Average δE	-20.2 %

Table: Average bias δE of the events in the 4 classes.

Focus on type D events

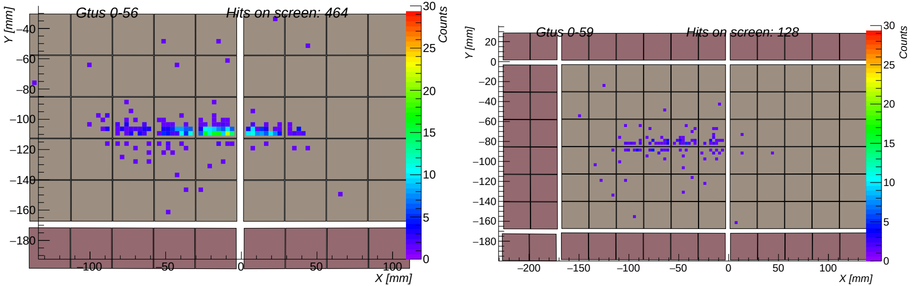

Figure: Some simulated $E = 1 \times 10^{20}\,\mathrm{eV}$ and $\theta = 60$ degrees events that are "badly" reconstructed. These events are parallel or almost parallel to PMTs gaps, so the signal is reduced.

BIASES IN E_{RECO} -FITS OPTIMIZATION

Non-optimal automatic fitting procedure

Event 16 is classified as D because of the automatic fitting:

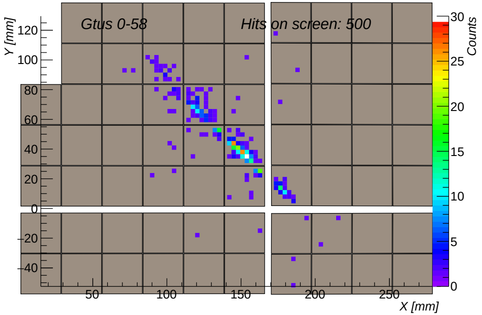

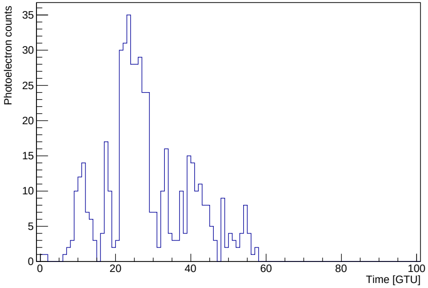

Figure: Simulated $E = 1 \times 10^{20}\,\mathrm{eV}$ and $\theta = 60$ degrees event. Left: Image of the shower and the focal surface of the detector. Right: Photelectron counts curve as a function of time (GTU).

$\rightarrow$ Reconstructed energy is $E_{reco} = 3 \times 10^{19}\,\mathrm{eV}$.

Non-optimal automatic fitting procedure

Event 16 is classified as D because of the automatic fitting:

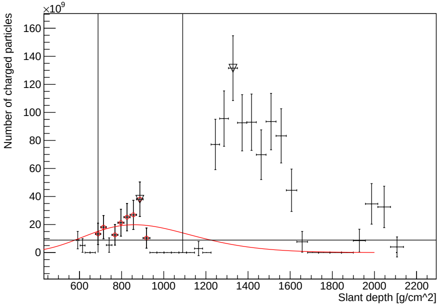

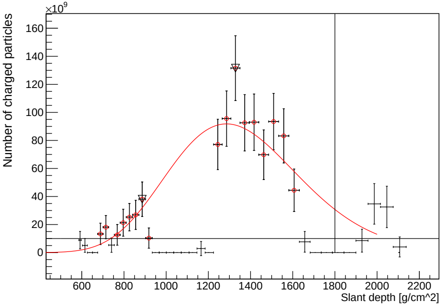

Figure: Left: Fit from the algorithm. Right: Fit with different boundary lines chosen "by hand". $E_{reco} = 1.3 \times 10^{20}\,\mathrm{eV}$, the error on energy reconstruction is reduced.

Fortunately these events are easily recognisable and an improved choice of the fit boundaries can be made.

Fits optimization

Event per event correction:

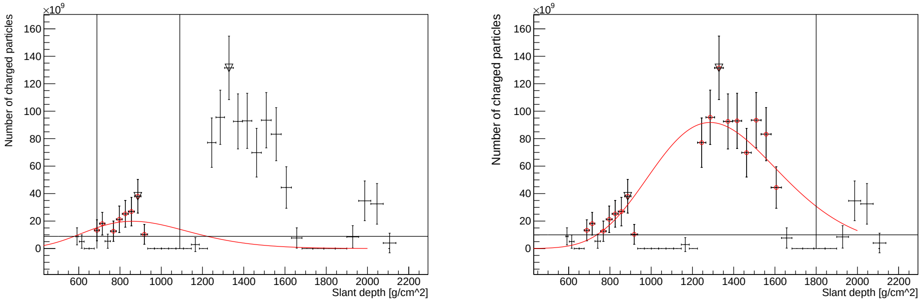

Figure: Left: Fit from the algorithm. $E_{reco} = 3 \times 10^{19}\,\mathrm{eV}$. Right: Optimized fit with different boundaries. $E_{reco} = 1.3 \times 10^{20}\,\mathrm{eV}$. Bias from negative to positive.

Fits optimization

Event per event correction:

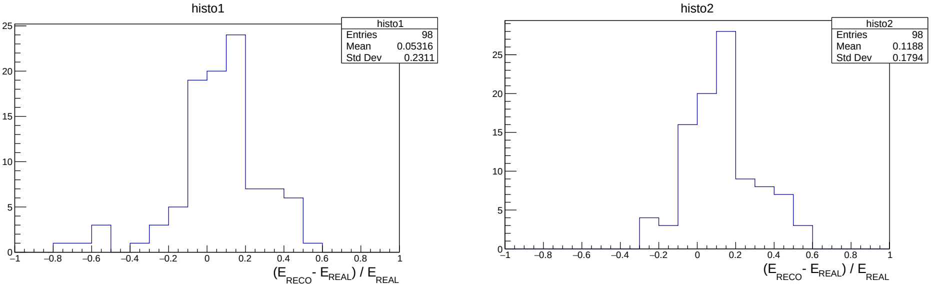

Figure: Left: $(E_{\mathrm{reco}} - E_{\mathrm{real}})/E_{\mathrm{real}}$ distribution of the 100, $1 \times 10^{20}\,\mathrm{eV}$, 60 degrees events simulated in the center considered before, without corrections. Right: Same sample, but with the optimization of the fits boundaries when needed.

Bias from 5% to 12%.

Fits optimization

If we consider histograms in Fig. 17:

- Negative bias is corrected (no more events with $< -30\%$ relative error)
- Positive bias is not corrected (more events with $> +20\%$ relative error)

So positive bias remains (and increases).

The fits of the events with high positive biases are good.
So why the energy reconstruction is bad?

The problem is that the geometry is not well reconstructed:

1. X_{max} is reconstructed too deep
2. Overestimation of photon counts
3. Overestimation of E_{reco}

And PMTs/PDMs gaps that cause signal loss.

Overestimated E_{reco}

Examples of non-optimized fits with overestimated E_{reco}:

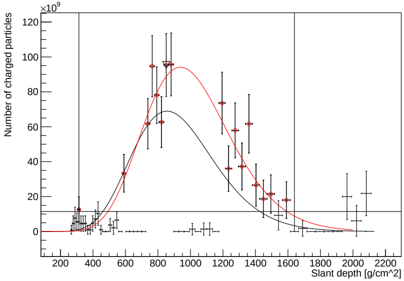

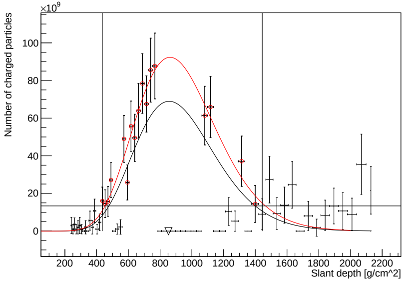

Figure: The fit line is in red, the reconstructed points are in red/black with black error bars and the simulated points are presented with a black line. Left: $E_{reco} = 1.55 \times 10^{20}\,\mathrm{eV}$. Right: $E_{reco} = 1.4 \times 10^{20}\,\mathrm{eV}$.

The fits are good with no need of optimization. But E_{reco} is overestimated. Clearly the reconstructed points are higher than the simulation.

Overestimated E_{reco}

Example of optimized fit with overestimated E_{reco}:

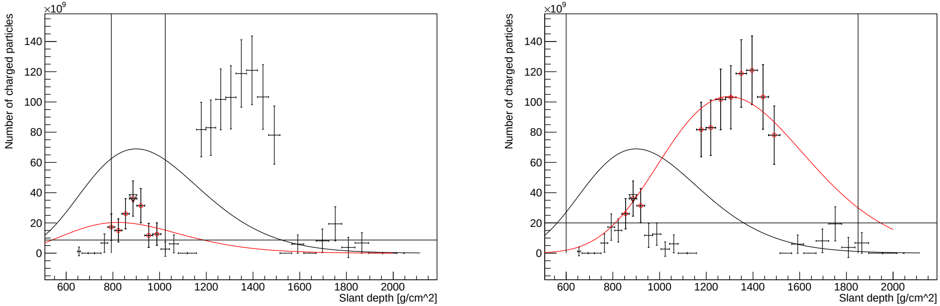

Figure: The fit line is in red, the reconstructed points are in red/black with black error bars and the simulated points are presented with a black line. Left: Non-optimized fit, $E_{reco} = 3 \times 10^{19}\,\mathrm{eV}$. Right: Optimized fit, $E_{reco} = 1.5 \times 10^{20}\,\mathrm{eV}$.

The fit after the corrections is good. But E_{reco} is overestimated. Clearly the reconstructed points are far from the simulation.

BIASES IN E_{RECO} -TEST WITH FIXED GEOMETRY

Reconstruction with fixed geometry

Reconstruction with fixed geometry:

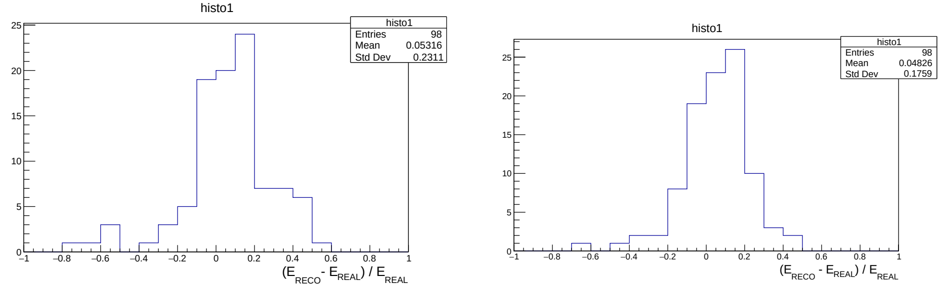

Figure: Left: $(E_{\mathrm{reco}} - E_{\mathrm{real}})/E_{\mathrm{real}}$ distribution of the 100, $1 \times 10^{20}\,\mathrm{eV}$, 60 degrees events simulated in the center, without any corrections. Right: Same sample, but with a more correct reconstruction because the geometry of the event is fixed.

Positive bias reduced (better estimation of the X_{max}).

Reconstruction with fixed geometry

Some examples:

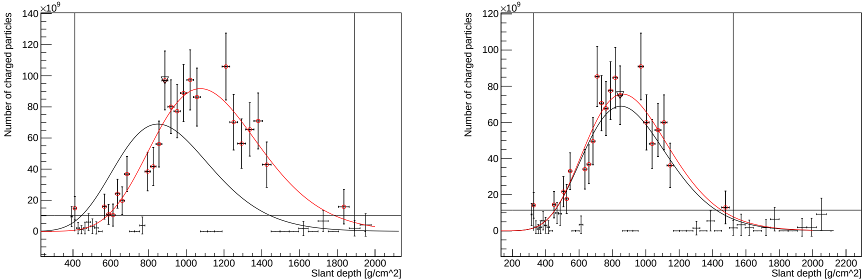

Figure: The fit line is in red, the reconstructed points are in red/black with black error bars and the simulated points are presented with a black line. Left: Before fixed geometry, $E_{reco} = 1.33 \times 10^{20}\,\mathrm{eV}$. Right: After fixed geometry, $E_{reco} = 1.1 \times 10^{20}\,\mathrm{eV}$

Reconstruction with fixed geometry + fits optimization

Reconstruction with fixed geometry and fits optimization:

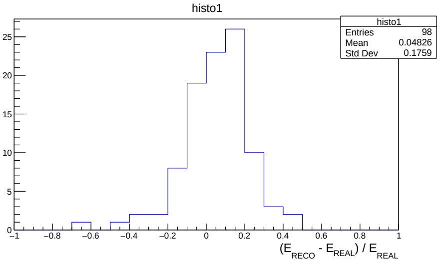

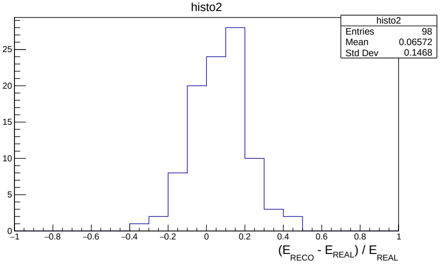

Figure: Left: $(E_{\mathrm{reco}} - E_{\mathrm{real}})/E_{\mathrm{real}}$ distribution of the 100, $1 \times 10^{20}\,\mathrm{eV}$, 60 degrees events simulated in the center, without fits corrections, but reconstruction with fixed geometry. Right: Same sample, but with the optimization of the fits boundaries when needed plus reconstruction with fixed geometry.

- With fixed geometry: right tail reduced
- With fixed geometry and fits optimization: left tail also reduced

BIASES IN E_{RECO} -GAPS EXAMPLES

Problematic events - 13

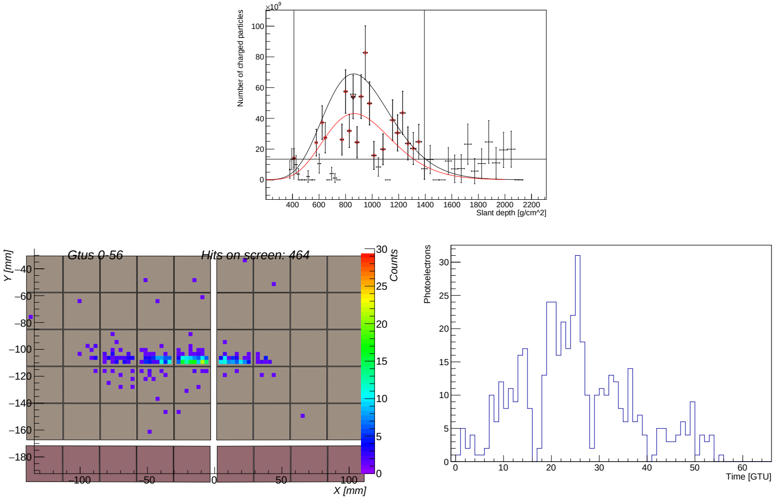

Figure: $E_{reco} = 6 \times 10^{19}\,\mathrm{eV}$.

Problematic events - 37

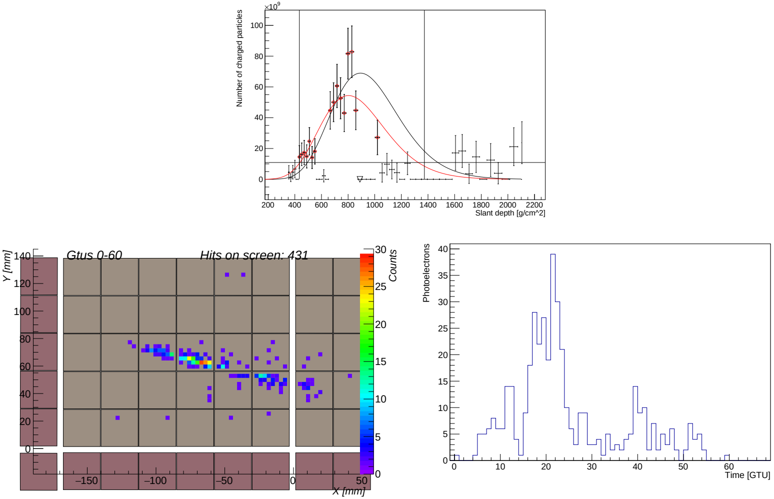

Figure: $E_{reco} = 8 \times 10^{19}\,\mathrm{eV}$.

ENERGY RECO

K-EUSO energy reconstruction performance

- 2500 showers simulated in the center of the detector
- Fixed conditions: $E = 1 \times 10^{20}\,\mathrm{eV}$, $\theta = 60°$

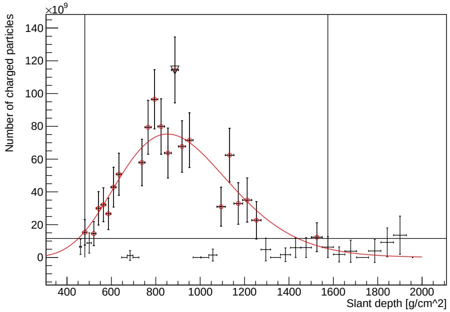

1. Black crosses: reconstructed shower profile as a function of slant depth
2. Red line: shower profile fit $\longrightarrow$ parameters are E and X_{max}
3. Reconstructed energy is $1.1 \times 10^{20}\,\mathrm{eV}$

Energy resolution (center)

Center of the field of view

Energy [eV]	Zenith angle [°]	Energy resolution [%]
5×10^{19}	30	27.2
5×10^{19}	45	25.4
5×10^{19}	60	21.0
5×10^{19}	75	14.7
7×10^{19}	30	26.4
7×10^{19}	45	25.3
7×10^{19}	60	19.6
7×10^{19}	75	13.4
1×10^{20}	30	26.5
1×10^{20}	45	24.0
1×10^{20}	60	19.0
1×10^{20}	75	12.7

Energy resolution (full field of view)

Full field of view

Energy [eV]	Zenith angle [°]	Energy resolution [%]
5×10^{19}	30	25.2
5×10^{19}	45	24.7
5×10^{19}	60	21.8
5×10^{19}	75	15.7
7×10^{19}	30	26.8
7×10^{19}	45	24.4
7×10^{19}	60	20.3
7×10^{19}	75	13.7
1×10^{20}	30	26.6
1×10^{20}	45	24.4
1×10^{20}	60	19.8
1×10^{20}	75	13.1

X_{MAX} **RECO**

Exclusion of events in the tails of the distribution

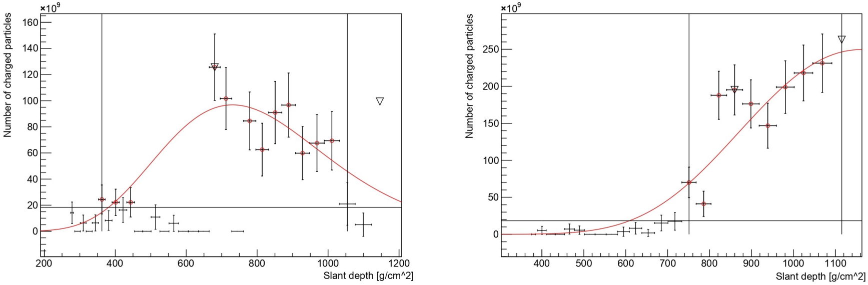

1. Left: Events in the left tail. These events are affected by huge gaps. Gaps removal test: left tail is reduced.
2. Right: Events in the right tail. These events impact on the ground before the maximum development of the shower and this affects X_{max} reconstruction. Gaps removal test: right tail is not reduced, proves that this is a problem of the geometry of the event.

X_{max} reconstruction - $1 \times 10^{20}\,\mathrm{eV}$, 45° examples

- 4500 showers simulated in the center at fixed energies and zenith angles
- Fixed conditions: $E = 2 \times 10^{20}\,\mathrm{eV}$, $\theta = 30^\circ$
- X_{max} reconstruction with Cherenkov method
- X_{max} resolution: standard deviation of the $(X_{max,real} - X_{max,reco})$ distribution (central peak)

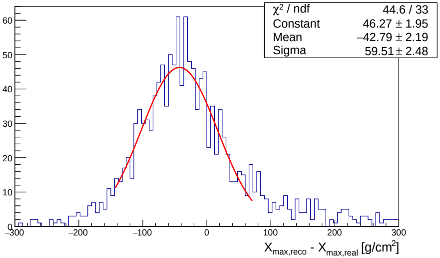

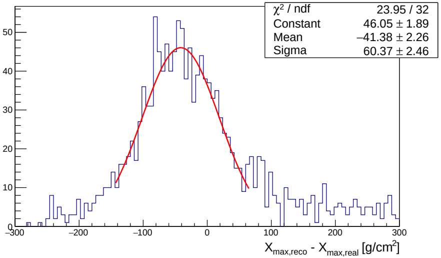

Figure: Estimation of the X_{max} resolution for a $2 \times 10^{20}\,\mathrm{eV}$, 45 degrees event simulated in the center of the detector (left) and in the full field of view (right).

X_{max} reconstruction - $2 \times 10^{20}\,\mathrm{eV}$, 30° example

Gaps removal test:

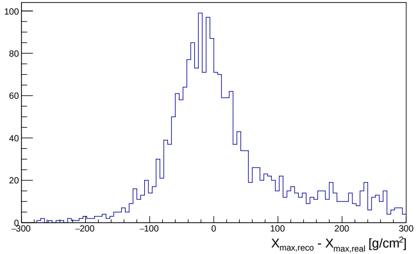

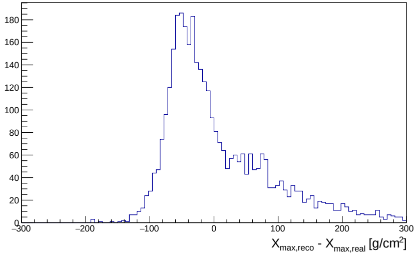

Figure: $(X_{max,reco} - X_{max,real})$ distribution of a $2 \times 10^{20}\,\mathrm{eV}$, 30 degrees event simulated in the center. On the left: Standard case. On the right: Reduced PMTs gaps.

$\longrightarrow$ Right tail remains, events that impact on the ground not affected by gaps removal.

X_{max} reconstruction - $2 \times 10^{20}\,\mathrm{eV}$, 45° example

Gaps removal test:

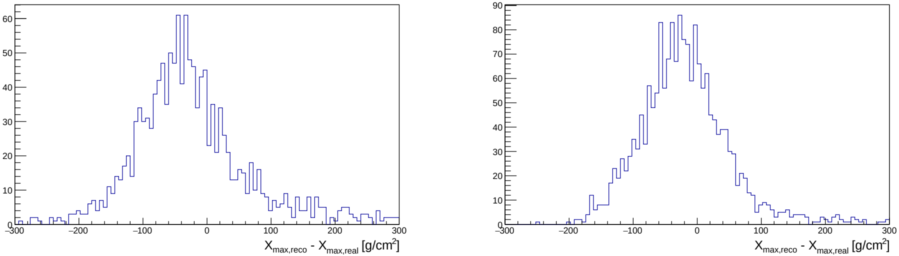

Figure: $(X_{max,reco} - X_{max,real})$ distribution of a $2 \times 10^{20}\,\mathrm{eV}$, 45 degrees event simulated in the center. On the left: Standard case. On the right: Reduced PMTs gaps.

$\longrightarrow$ Different geometry, resolutive for both tails.

MINI-EUSO

Mini-EUSO trigger efficiency in uniform/disuniform bg

- Study of Mini-EUSO L1 trigger efficiency in uniform/disuniform background $\rightarrow$ relevant for future space-based experiments like K-EUSO
- 1 count/pixel/GTU, $\sim$ 500 photons per m^2srns (average)
- $\eta_Q = 0.27$ (average)

Disuniform background

- Obtained in ESAF by simply re-scaling the η_Q of each pixel
- But disuniformity may be due to clouds/different geographical conditions

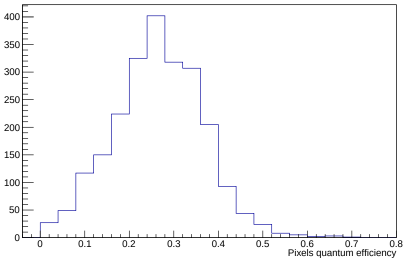

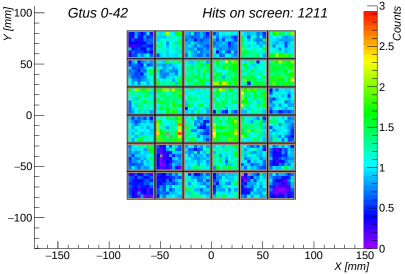

Mini-EUSO trigger efficiency in uniform/disuniform bg

- $N = 10^4$ showers, $E = 10^{20} - 10^{21}$eV, $\theta = 0° - 90°$
- $\epsilon(E) = \frac{N_{trigg}}{N_{simu}}(E)\frac{A_{simu}}{A_{fov}}$
- Fit with error function: $\epsilon(E) \sim \frac{1}{2}[1 + erf(\frac{log_{10}(E/eV) - p_0}{p_1})]$

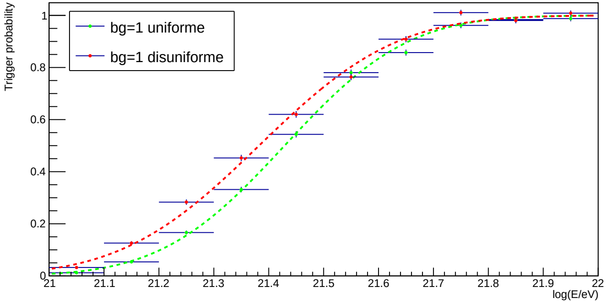

- Threshold: $E_{th} \sim 2.5 \times 10^{21}$ eV (uniform) vs $E_{th} \sim 2 \times 10^{21}$ eV (disuniform)
- Plateau: $E_{Full} \sim 6 \times 10^{21}$ eV

Mini-EUSO - disuniform background

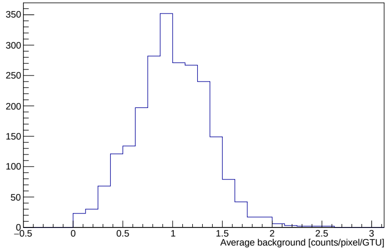

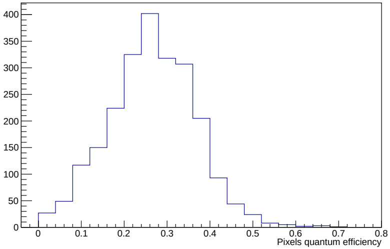

Mini-EUSO bg = 2

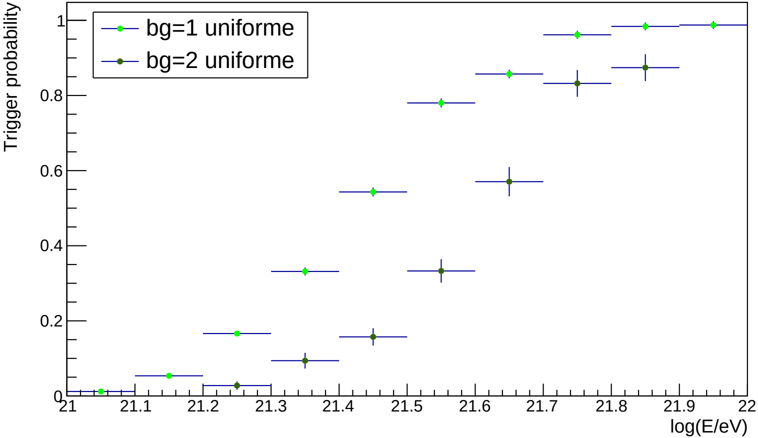

Mini-EUSO bg = 2

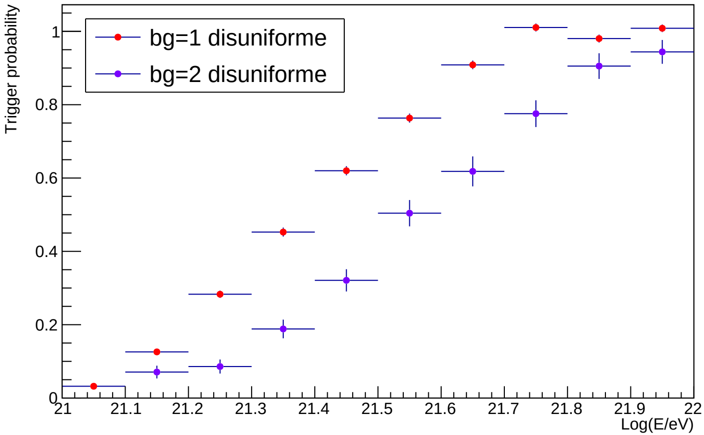

MINI-EUSO - KTH

Mini-EUSO trigger efficiency vs bg counts

Energy threshold (E_{th}) = 50% of trigger efficiency

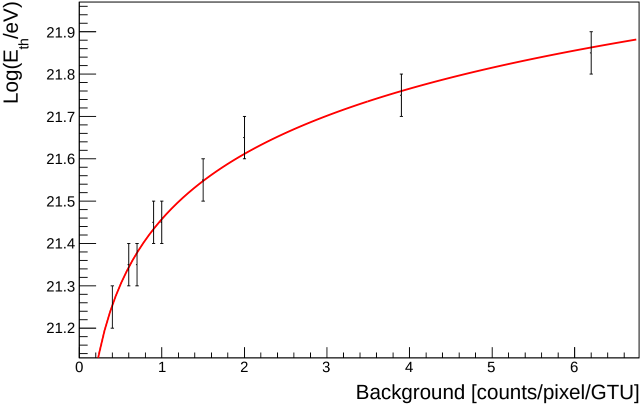

→ E_{th} scales with the square root of the background

Selection of particular bg conditions from data

Condition	Bg [counts/pixel/GTU]*
Clear land, no moon	0.7
Clear seas, no moon	0.9
Cloudy land/seas, no moon	1.5
Clear land/seas, half moon	2

*Peak values

Mini-EUSO trigger efficiency in different bg conditions

Trigger efficency/probability: $\epsilon(E) = \frac{N_{trigg}}{N_{simu}}(E) \times \frac{A_{simu}}{A_{fov}}$

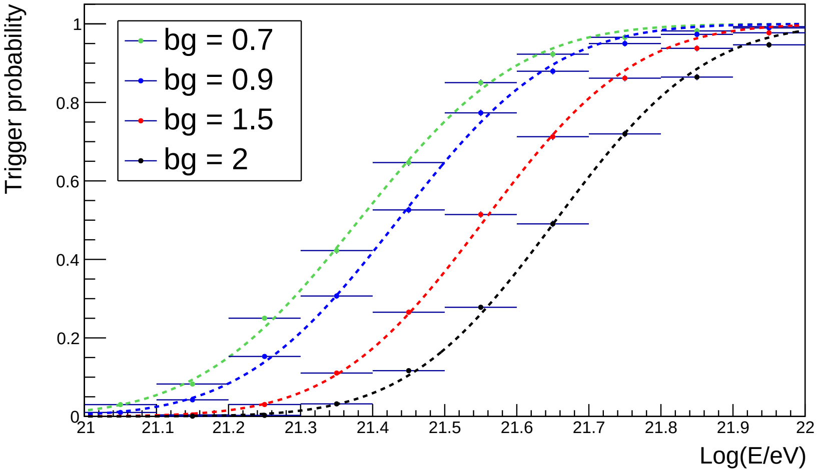

Mini-EUSO annual exposure

Exposure:

$$\mathcal{E}(E) = \mathcal{A}(E) \times \eta \times \eta_{clouds} \times \eta_{city} \times t$$

$\longrightarrow$ $\mathcal{A}$ is the geometrical aperture
$\longrightarrow$ t is Mini-EUSO active time ($= 216h/year$) $\times$ time fraction
$\longrightarrow$ η (~ 0.3) is the astronomical duty cycle
$\longrightarrow$ η_{city} ($\sim$ 0.9) and η_{clouds} ($\sim$ 0.7) take into account urban areas and clouds coverage

Mini-EUSO annual exposure

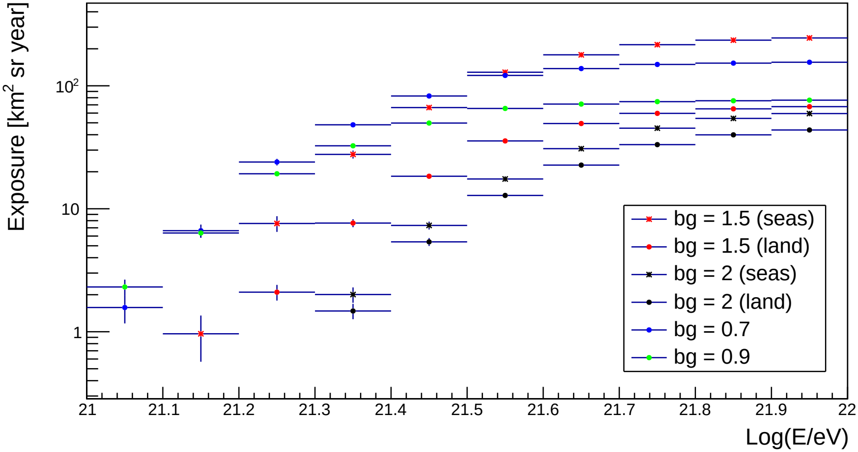

$\longrightarrow$ The terms are different because of the background that affects the trigger efficiency and the η and the t that are in the Eq. for the exposure

Mini-EUSO annual exposure

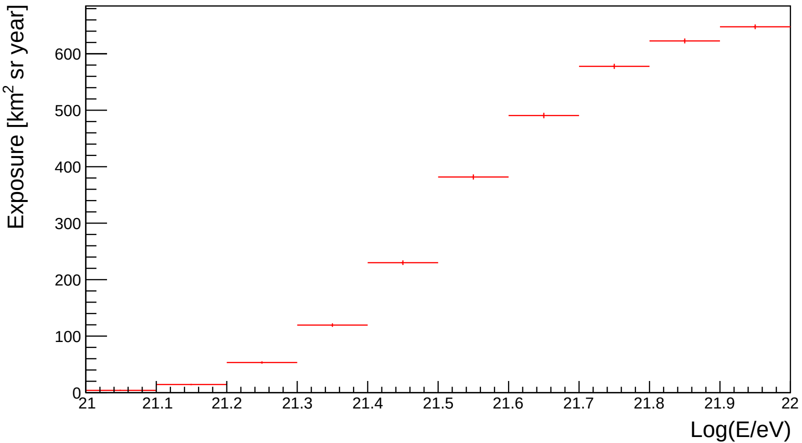

$\longrightarrow$ Summing all the terms, $\mathcal{E} \sim 660\,\mathrm{km}^2$ sr year at the plateau